



# Molecular Structures and Antiviral Activities of Naturally Occurring and Modified Cassane Furanoditerpenoids and Friedelane Triterpenoids from *Caesalpinia minax*

Ren-Wang Jiang,<sup>a</sup> Shuang-Cheng Ma,<sup>b</sup> Zhen-Dan He,<sup>b</sup> Xue-Song Huang,<sup>c</sup>  
Paul Pui-Hay But,<sup>b</sup> Hua Wang,<sup>b</sup> Siu-Pang Chan,<sup>a</sup> Vincent Eng-Choon Ooi,<sup>b</sup>  
Hong-Xi Xu<sup>b</sup> and Thomas C.W. Mak<sup>a,\*</sup>

<sup>a</sup>Department of Chemistry & Institute of Chinese Medicine, The Chinese University of Hong Kong, Hong Kong SAR, PR China

<sup>b</sup>Department of Biology & Institute of Chinese Medicine, The Chinese University of Hong Kong, Hong Kong SAR, PR China

<sup>c</sup>College of Food Science and Engineering, Shandong Agricultural University, Taian, Shan Dong, PR China

Received 21 December 2001; accepted 9 February 2002

**Abstract**—Further investigation of the active components of the chloroform fraction of the seeds of *Caesalpinia minax* led to the isolation of a new cassane furanoditerpenoid, caesalmin H (**1**), together with two known furanoditerpenoid lactones, caesalmin B (**2**) and bonducellpin D (**3**). Reduction of the naturally abundant caesalmin D (**9**), E (**10**) and F (**11**) resulted in three new furanoditerpenoid derivatives **4–6**. Phytochemical study of the stem of the same plant and subsequent reduction afforded two friedelane triterpenoids (**7–8**), which were identified by spectroscopic methods. Compounds **1–2** and **4–8** were corroborated by single crystal X-ray analysis. The factors governing the reduction of cassane furanoditerpenoids and friedelane triterpenoids were investigated by correlating the crystallographic results with density functional theory. The inhibitory activities of **2–8** on the Para3 virus were evaluated by cytopathogenic effects (CPE) reduction assay. © 2002 Elsevier Science Ltd. All rights reserved.

## Introduction

Natural products have proven to be a rich source of biologically active materials and potentially useful lead to drug development.<sup>1</sup> Motivated by the severe health hazards worldwide caused by respiratory infections, and the pronounced resistance from some pathogens to currently administered therapeutic agents,<sup>2</sup> we started a program to develop antiviral agents from natural sources. Following a lead based on ethanomedical usage,<sup>3</sup> we investigated the bioactive components of the seeds of *Caesalpinia minax* Hance. The results showed that the tetracyclic furanoditerpenoids (caesalmin C, D, E and F) from the brown precipitate after defatting with hexane possessed potent anti-para3 (para-influenza virus type 3) activity.<sup>4</sup>

Further investigation of the chloroform fraction resulted in the isolation of a new furanoditerpenoid, named caesalmin H (**1**), together with caesalmin B (**2**)<sup>5</sup> and bonducellpin D (**3**).<sup>6</sup> Reduction of the naturally abundant caesalmin D (**9**), E (**10**) and F (**11**)<sup>4</sup> yielded three new

furanoditerpenoid derivatives, that is, 1 $\alpha$ ,5 $\alpha$ ,14 $\alpha$ -trihydroxy-6 $\alpha$ ,7 $\beta$ -diacetoxyvouacapane (**4**), 1 $\alpha$ ,5 $\alpha$ ,6 $\alpha$ ,7 $\beta$ ,14 $\beta$ -pentahydroxyvouacapane (**5**) and 1 $\alpha$ ,5 $\alpha$ -dihydroxy-14 $\beta$ -methoxy-6 $\alpha$ ,7 $\beta$ -diacetoxyvouacapane (**6**). In addition, investigation of the chemical components of the stem of *C. minax* led to the isolation of a friedelane triterpenoid, that is, friedelin (**7**),<sup>7</sup> and a reduction experiment was performed to afford epifriedelinol (**8**)<sup>8</sup> (Fig. 1). We report herein the structure elucidation of the above compounds and their antiviral activities against Para3 virus, a major pathogen of some respiratory infections.<sup>9</sup> Detailed knowledge about the molecular geometry is often necessary for relating biological activity to structure, exploring potential clinical and chemical uses, and as a starting point for further explorations using molecular modeling. Thus X-ray crystallographic studies on compounds **1–2** and **4–8** were performed for both molecular structure determination and further optimization.

## Results and Discussion

High-resolution liquid secondary ion mass spectrometry (HRLSIMS) of (**1**) suggested the molecular formula C<sub>22</sub>H<sub>32</sub>O<sub>5</sub> which agrees well with the molecular ion *m/z*

\*Corresponding author. Tel.: +852-2609-6279; fax: +852-2603-5057; e-mail: tcwmak@cuhk.edu.hk

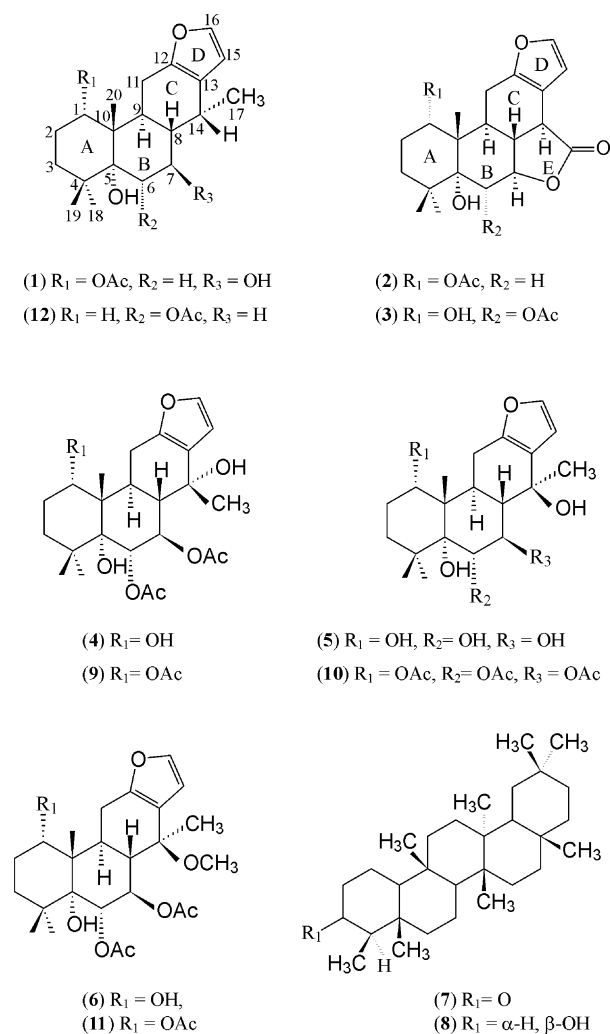


**Figure 1.** Structural formulae of some cassane furanoditerpenes and friedelane triterpenoids.

376 obtained from EIMS. A color change to reddish purple with the Ehrlich reagent, in combination with a fragment ion peak at  $m/z$  108 [ $\text{C}_7\text{H}_8\text{O}$ ] $^+$  derivable from characteristic reverse Diels–Alder cleavage of the furan moiety, indicated a furanoid structure, which was also substantiated by a pair of doublets at  $\delta$  6.22 (1H, d,  $J=1.0$  Hz, H-15) and  $\delta$  7.24 (1H, d,  $J=1.0$  Hz, H-16) and four  $sp^2$  carbon atoms at  $\delta$  148.25 (C-12, s), 122.04 (C-13, s), 109.68 (C-15, d) and 140.60 (C-16, d). The  $^{13}\text{C}$  NMR resonance at  $\delta$  168.82 (C-21, s) and the infrared peak at  $1740\text{ cm}^{-1}$  revealed the presence of a carbonyl group (Tables 1 and 2). Accordingly, four of the seven degrees of unsaturation suggested by the molecular formula can be ascribed to the furan ring and the carbonyl group, and the three remaining degrees of unsaturation account for the tricycyclic system. Thus **1** was inferred to possess a cassane-type furanoditerpenoid skeleton.

The  $^{13}\text{C}$  and DEPT NMR spectra, indicating the presence of 17  $sp^3$  carbon atoms (5 methyls, 4 methylenes, 5 methines and 3 quaternary carbons), four  $sp^2$  carbons (2 methines and 2 quaternary carbons) and a carbonyl group, confirmed the molecular skeleton of **1**. The presence of the carbonyl group and an oxygenated carbon at  $\delta$  75.82 (C-1, d) can be attributed to an acetate group, which is supported by the methyl signal  $\delta$  2.10 (3H, s, H<sub>3</sub>-22), and its position at C-1 was confirmed by the HMBC spectrum which showed that H-1 ( $\delta$  4.91, br. s) is correlated to C-2, C-3, C-5, C-10, C-20 and the acetate carbonyl attached to C-1. The other two C–O signals [ $\delta$  78.59 (C-5, s) and 67.79 (C-7, d)] must be due to hydroxyl groups which were supported by the absorption band ( $3586\text{ cm}^{-1}$ ) in the IR spectrum. Normally, all furanoditerpenoids isolated from *Caesalpinia* genus so far possess an  $\alpha$ -oriented hydroxyl group at C-5, and thus the presence of 5-OH can be speculated from the biogenetic view point. Another 7-OH group was confirmed by the HMBC spectrum which showed that H-7

**Table 1.**  $^1\text{H}$  NMR data of compounds **1**, **4**, **5** and **6** (300 MHz, in  $\text{CD}_3\text{OD}$ )

Position	<b>1</b>	<b>4</b>	<b>5</b>	<b>6</b>
1	4.91, 1H, br s	3.77, 1H, br s	3.66, 1H, br s	3.66, 1H, br s
2	1.64, 1H, m, 2-H $^\alpha$ 1.92, 1H, m, 2-H $^\beta$	1.63, 1H, m, 2-H $^\alpha$ 1.89, 1H, m, 2-H $^\beta$	1.59, 1H, m, 2-H $^\alpha$ 1.92, 1H, m, 2-H $^\beta$	1.64, 1H, m, 2-H $^\alpha$ 1.93, 1H, m, 2-H $^\beta$
3	1.41, 1H, m, 3-H $^\alpha$ 1.96, 1H, m, 3-H $^\beta$	1.01, 1H, m, 3-H $^\alpha$ 1.65, 1H, m, 3-H $^\beta$	1.00, 1H, m, 3-H $^\alpha$ 1.61, 1H, m, 3-H $^\beta$	1.05, 1H, m, 3-H $^\alpha$ 1.68, 1H, m, 3-H $^\beta$
6	1.76, 2H, m	5.49, 1H, d, 8.4	3.82, 1H, d, 9.0	5.44, 1H, d, 8.1
7	4.71, 1H, dt, 5.3, 12.9	5.86, 1H, dd, 8.4, 8.8	4.17, 1H, dd, 9.0, 10.5	5.64, 1H, dd, 8.1, 8.7
8	2.13, 1H, ddd, 4.2, 10.4, 12.9	2.09, 1H, m	2.02, 1H, m	2.08, 1H, m
9	2.67, 1H, ddd, 5.1, 8.1, 10.4	3.17, 1H, dt, 5.1, 11.5	2.85, 1H, ddd, 4.5, 6.3, 10.2	2.97, 1H, ddd, 5.7, 7.8, 11.1
11	2.28, 1H, dd, 5.1, 16.4, 11-H $^\alpha$ 2.44, 1H, dd, 8.1, 16.4, 11-H $^\beta$	2.78, 1H, dd, 5.1, 15.9, 11-H $^\alpha$ 2.42, 1H, dd, 11.5, 15.9, 11-H $^\beta$	2.64, 1H, dd, 6.3, 16.3, 11-H $^\alpha$ 2.45, 1H, dd, 10.8, 16.2, 11-H $^\beta$	2.74, 1H, dd, 5.7, 15.8, 11-H $^\alpha$ 2.46, 1H, dd, 11.1, 15.8, 11-H $^\beta$
14	3.11, 1H, m			
15	6.22, 1H, d, 1.0	6.42, 1H, d, 2.0	6.40, 1H, d, 2.0	6.23, 1H, d, 1.6
16	7.24, 1H, d, 1.0	7.29, 1H, d, 2.0	7.29, 1H, d, 2.0	7.24, 1H, d, 1.6
17	1.11, 3H, d, 5.4	1.41, 3H, s	1.47, 3H, s	1.49, 3H, s
18	1.12, 3H, s	1.14, 3H, s	1.24, 3H, s	1.15, 3H, s
19	1.14, 3H, s	1.08, 3H, s	1.08, 3H, s	1.09, 3H, s
20	1.07, 3H, s	1.17, 3H, s	1.28, 3H, s	1.19, 3H, s
1-OAc	2.10, 3H, s			
6-OAc		1.96, 3H, s		2.00, 3H, s
7-OAc		2.03, 3H, s		2.05, 3H, s
14-OCH <sub>3</sub>				3.04, 3H, s

**Table 2.**  $^{13}\text{C}$  NMR data of compounds **1**, **4**, **5** and **6** (75 MHz, in  $\text{CD}_3\text{OD}$ )

Position	<b>1</b>	<b>4</b>	<b>5</b>	<b>6</b>
1	75.82 d	68.60 d	72.68 d	73.18 d
2	21.56 t	22.40 t	22.04 t	23.19 t
3	30.03 t	32.45 t	32.47 t	32.56 t
4	38.50 s	38.89 s	39.14 s	38.94 s
5	78.59 s	80.14 s	80.69 s	80.91 s
6	22.55 t	72.52 d	74.38 d	73.77 d
7	67.79 d	72.52 d	75.57 d	76.23 d
8	42.56 d	33.93 d	35.12 d	38.22 d
9	35.37 d	33.93 d	35.12 d	35.69 d
10	43.47 s	44.32 s	44.70 s	45.12 s
11	22.07 t	25.49 t	25.59 t	23.76 t
12	148.25 s	150.94 s	149.35 s	151.80 s
13	122.04 s	123.58 s	124.28 s	122.10 s
14	31.93 d	77.10 s	73.28 s	78.78 s
15	109.68 d	107.98 d	107.52 d	108.37 d
16	140.60 d	150.94 d	141.75 d	142.33 d
17	28.18 q	30.56 q	31.23 q	31.10 q
18	27.42 q	27.80 q	25.58 q	25.93 q
19	25.28 q	24.62 q	24.77 q	25.35 q
20	17.17 q	16.44 q	16.40 q	17.47 q
1-OAc	168.82 s			
	17.84 q			
6-OAc		171.78 s		170.74 s
		21.05 q		21.97 q
7-OAc		171.78 s		171.68 s
		21.05 q		22.37 q

$^{13}\text{C}$  multiplicities were determined using the DEPT pulse sequences.

( $\delta$  4.71, dt,  $J = 5.3, 12.9$  Hz) is correlated to C-5, C-6, C-8, C-9 and C-14. The 17-methyl appeared as a doublet at  $\delta$  1.11 (3H, d,  $J = 5.4$  Hz) which indicated that C-14 is a non-oxygenated carbon as found in caesaldekarin A (**12**, Fig. 1), which was isolated from *Caesalpinia major*.<sup>10</sup> Compound **1** is the first tetracyclic furanoditerpenoid from *C. minax* that possesses a 17-methyl attached to a non-oxygenated C-14.

The molecular structure and relative configuration of **1** were established unambiguously by X-ray crystallographic analysis as 5 $\alpha$ ,7 $\beta$ -dihydroxy-1 $\alpha$ -acetoxyvouacapanone (Fig. 2a). The asymmetric unit consists of two independent molecules of **1** (designated as **I** and **II**) and a water molecule disordered over two sites (occupancy 0.3 and 0.7). The two independent molecules are connected by a pair of hydrogen bonds involving the hydroxyl group at C-7 as both hydrogen-bond donor and acceptor, that is, O-4-H $\cdots$ O-4' (2.920 Å) and O-4'-H $\cdots$ O-4 (2.920 Å). The two water sites are linked to compound (**I**) by hydrogen bonds O<sub>2</sub>1w $\cdots$ O-4' (2.889 Å,  $x, 1+y, z$ ) and O-2w $\cdots$ O-2' (3.045 Å,  $0.5+x, 1.5-y, -z$ ) (Fig. 2b), respectively. The two independent molecules take the same conformation except that the acetate group exhibits larger thermal motion in **II** than in **I** (the displacements of O-2, C-21 and C-22 for **I** are 0.086, 0.051 and 0.071, respectively, and for **II** are 0.123, 0.103 and 0.120, respectively), indicating a significant degree of librational disorder<sup>11</sup> (Table S1, see supplementary material). The thermal motion of the acetate group led to slightly different orientations as indicated by the torsion angle of C-1-O-1-C-21-O-2 ( $-4.7^\circ$  for **I** and  $2.0^\circ$  for **II**). Cyclohexane rings A and B adopt a chair conformation, while ring C exists as a twisted half-chair due to fusion to the planar furan ring D.

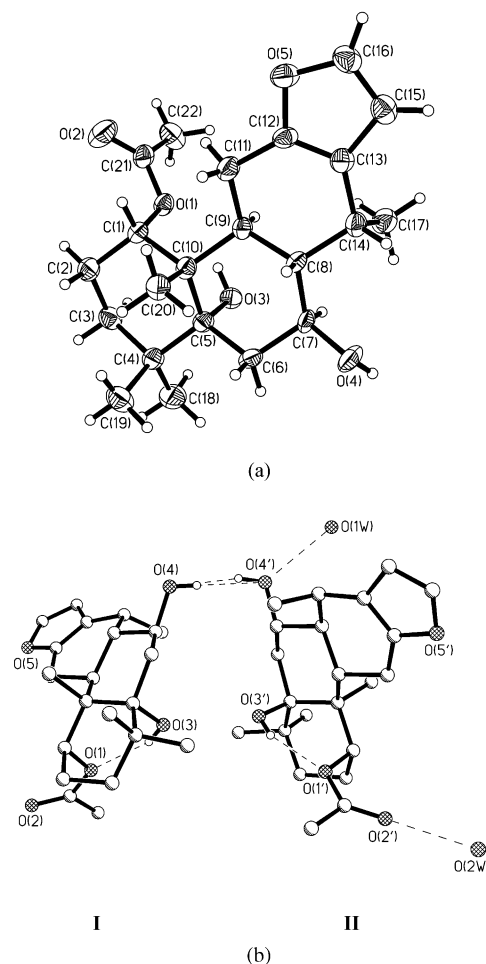


**Figure 2.** (a) Molecular structure of **1** with atom labeling scheme. The C and O atoms are drawn as 30% thermal ellipsoids. (b) Perspective view showing the asymmetric unit of 2(**I**)·H<sub>2</sub>O, including hydrogen atoms involved in hydrogen bonds, which are represented by dashed lines. Two independent molecules of **1** (designated as **I** and **II**) forming a hydrogen-bonded dimer.

Cassane furanoditerpenoids, also named 'vouacapanone', are characterized by the fusion of the tricycyclic ring with a furan ring. Such a nucleus is mostly distributed in the genera *Caesalpinia*<sup>12</sup> and *Pterodon*<sup>13</sup> of the same family (Fabaceae),<sup>14</sup> and differentiated by the presence of a C-5 oxygenated group in the former genus. Examination of the previously reported cassane furanoditerpenoids revealed three common structural features: (i) the three six-membered rings A, B and C are fused as a *trans-anti-trans* system; (ii) the substituents at C-1, C-5 and C-10 occupy axial positions and the substituents at C-6 and C-7 are equatorial; (iii) the hydroxyl group at C-5 forms an intramolecular hydrogen bond with the oxygenated group at C-1. Thus cassane furanoditerpenoids possess a highly stable and conserved skeleton. The absolute configurations of  $\epsilon$ -caesalpin<sup>15</sup> and compound **12**,<sup>10</sup> which share the same carbon skeleton with compound **1**, were well established by X-ray analysis using the anomalous dispersion method and comparison of the NMR data of MTPA derivatives, respectively. Accordingly, the absolute configuration of (**1**) can be inferred by considering the biogenetic relationship in the furanoditerpenoids, as shown in Figure 1.

Caesalmin B (**2**) was reported previously as its (2/1) solvate with acetone (triclinic, space group  $P1$ ) crystallized from a mixture of hexane/acetone (8:1).<sup>5</sup> Interestingly, it was also obtained here as a (3/1) hexane solvate (orthorhombic, space group  $P2_12_12_1$ ) from a different mixing ratio of the same solvents (hexane/acetone 20:1). The asymmetric unit consists of three independent molecules of **2** and a hexane molecule (Fig. 3). The conformations of the three molecules closely resemble one another and that in the triclinic form, that is, the A, B, C, D and E rings adopt chair, chair, twist-chair, planar and envelope conformations, respectively (Table S2, see supplementary material). The hexane molecules are arranged in an infinite chain along the  $a$ -axis. The shortest intermolecular contact with (**2**) being C-6'...O-3 (3.71 Å).

Pseudopolymorphism occurs when a compound co-crystallizes with different solvents or the same solvent but in different stoichiometric ratios.<sup>16</sup> Such phenomenon is common in host-guest systems<sup>17</sup> and also observed among natural products; for example, compound **9** has been found to crystallize as a methanol solvate and a hydrate, and stigmasterol forms both a monohydrate and a hemihydrate.<sup>4</sup> Compound **2** represents a rare example of pseudopolymorphism whereby the host selectively encloses different guests when the molar ratio of the two-component mixed solvent system is varied. The phenomenon of pseudopolymorphism highlights the role of solvent control in the organic molecular packing arrangement.

Bonducellpin D (**3**) was obtained as colorless needle-like crystals and identified as a cassane furanoditerpenoid lactone by comparing its physical and NMR data with the literature values.<sup>6</sup> Compound (**3**) had already been isolated from *Caesalpinia bonduc*;<sup>12b</sup> however, it was isolated from *C. minax* for the first time and it is the only furanoditerpenoid isolated from both plants. Attempts to obtain diffraction quality crystals of **3** were unsuccessful, although the crystal structures of similar lactones had been reported.<sup>5</sup>

Compound **4** was obtained by reduction of **9** with  $\text{LiAlH}_4$  in THF. The  $^1\text{H}$  and  $^{13}\text{C}$  NMR spectra are similar to those of **9** except for the absence of signals for

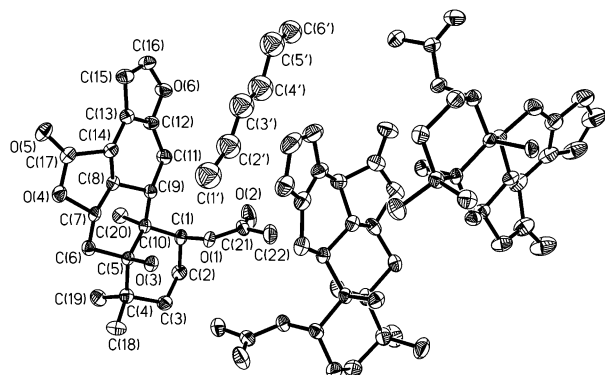


**Figure 3.** Perspective view showing the asymmetric unit of 3(**2**)· $\text{C}_6\text{H}_{14}$ . Only one of the two independent molecules of (**2**) and the hexane molecule are labeled.

the acetyl group at C-1 (**9**:  $\delta_{\text{H}}$ : 2.03, 3H, s and  $\delta_{\text{C}}$ : 169.88, s) and the high-field nature of H-1 (**4**:  $\delta_{\text{H}}$  3.77; **9**:  $\delta_{\text{H}}$  4.88). This information indicates that the acetyl group at C-1 had been reduced. The molecular structure of **4** was confirmed by X-ray analysis as  $1\alpha,5\alpha,14\alpha$ -trihydroxy- $6\alpha,7\beta$ -diacetoxyvouacapane (Fig. 4a). In the solid state, the intermolecular hydrogen bond O-1—H...O-4 ( $x, y-1, z, 2.873 \text{ \AA}$ ) links the molecules into a chain along the  $b$ -axis. Adjacent chains are cross-linked by another intermolecular hydrogen bond O-7—H...O-6 ( $1-x, y-0.5, -z, 2.920 \text{ \AA}$ ) (Fig. 4b).

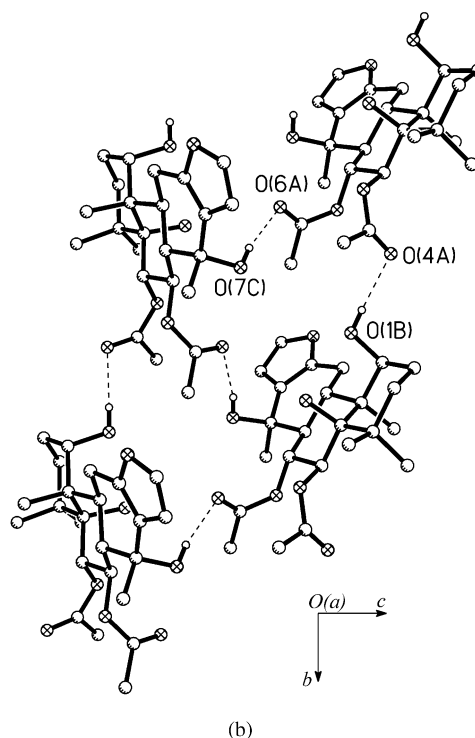
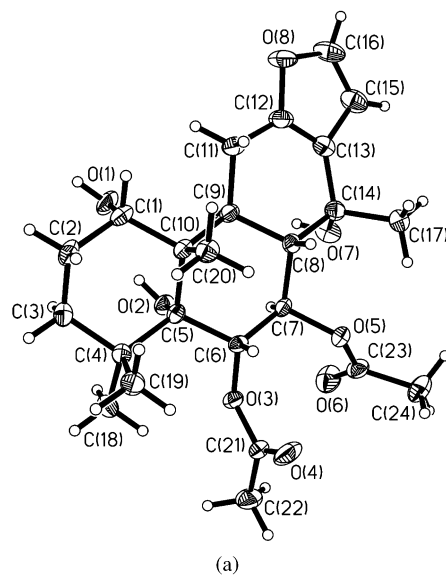


**Figure 4.** (a) Molecular structure of **4**. The C and O atoms are drawn as 30% thermal ellipsoids. (b) Hydrogen-bonding network of **4** viewed roughly down the  $a$ -axis. Selected hydrogen atoms highlight the scheme of hydrogen bonding.

Compound **5** was obtained by treatment of **10** with the same method as **9**. The  $^{13}\text{C}$  NMR spectra show only twenty diterpenoid skeleton carbon atoms and no signal for acetate carbonyl was observed. In the  $^1\text{H}$  NMR spectrum, signals for H-1, H-6 and H-7 were shifted to high-field (**5**:  $\delta_{\text{H}}$  3.66, 3.82 and 4.17; **10**:  $\delta_{\text{H}}$  4.84, 5.51 and 5.64). These data indicate that all three acetyl groups had been reduced. The molecular structure of **5** was confirmed by X-ray analysis as  $1\alpha,5\alpha,6\alpha,7\beta,14\beta$ -pentahydroxyvouacapane. The asymmetric unit consists of two same molecules of **5** and a water molecule which is located on the crystallographic 2-axis (Table S3, see supplementary material). The two molecules in the asymmetric unit are linked through three intermolecular hydrogen bonds, that is O-3–H $\cdots$ O-4' (2.708 Å), O-4'–H $\cdots$ O-3 (2.708 Å) and O-3'–H $\cdots$ O-4 (2.665 Å). The water molecule is connected to **5** through an intermolecular hydrogen bond O1w–H $\cdots$ O-5' (2.856 Å) (Fig. 5).

Compound **6** was obtained by reduction of **11** under the same conditions as **9** and **10**. Compound **6** gave a  $[\text{M}]^+$  peak at  $m/z$  464 corresponding for the molecular formula  $\text{C}_{25}\text{H}_{36}\text{O}_8$ . The absence of signals for the acetyl group at C-1 (**11**:  $\delta_{\text{H}}$ : 2.06, 3H, s and  $\delta_{\text{C}}$ : 170.93) and the high field nature of H-1 (**6**:  $\delta_{\text{H}}$  3.66; **11**:  $\delta_{\text{H}}$  4.86) indicated that the acetyl group at C-1 had been reduced to a hydroxyl group. The molecular structure of (**6**) was confirmed by X-ray analysis as  $1\alpha,5\alpha$ -dihydroxy-14 $\beta$ -methoxy-6 $\alpha,7\beta$ -diacetoxyvouacapane. A perspective view of the molecular structure is presented in Figure 6a. In the crystalline state, the intermolecular hydrogen bond O-1–H $\cdots$ O-4 ( $-x+1, y+1/2, -z+1/2, 2.817$  Å) links the molecules into a chain along the  $b$  direction. Adjacent chains are connected by a weak C–H $\cdots$ O interaction<sup>18</sup> (C-24–H $\cdots$ O-4, symmetry,  $-0.5+x, 0.5-y, -z, D=3.56$  Å,  $d=2.72$  Å and  $\theta=145.5^\circ$ ). Effectively, O-4 behaves as a bifurcated acceptor (Fig. 6b).

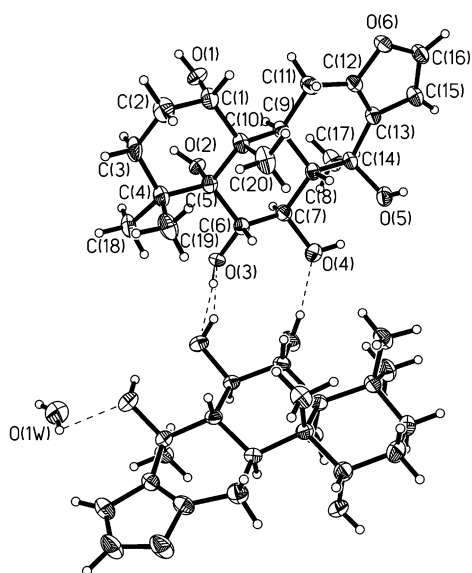


**Figure 5.** An ORTEP drawing (30% thermal ellipsoids) of  $2(\mathbf{5})\cdot 0.5\text{H}_2\text{O}$  showing the asymmetric unit. Only atoms in one of the two independent molecules is labeled. The intermolecular hydrogen bonds in the asymmetric unit are represented by dashed lines.

Compound **7** was isolated from the stem of *C. minax* and identified as the pentacyclic friedelane triterpene friedelin by comparison of its spectral and crystal data with the reported values.<sup>19</sup> Although friedelin (**7**) had been isolated from numerous plants,<sup>7</sup> it was isolated from the present source for the first time. Reduction of **7** with  $\text{LiAlH}_4$  resulted in compound **8**. In the  $^1\text{H}$  NMR spectrum, the oxygenated methine resonates at  $\delta$  3.73 (H-3, m). The width of the entire signal (8 Hz) indicates that the hydroxyl group should be  $\beta$ -oriented because the  $\alpha$ -oriented proton H-3, adopting the equatorial position, is split by two axial protons (H-2 $\alpha$  and H-4 $\alpha$ ) and an equatorial proton (H-2 $\beta$ ). As all three dihedral angles are close to  $60^\circ$ , the  $J$  values should be small (2–3 Hz). Accordingly, **8** is identified as epifriedelinol. The molecular structure of **8** was confirmed by X-ray analysis (Fig. 7). The crystal structure of **8** was reported

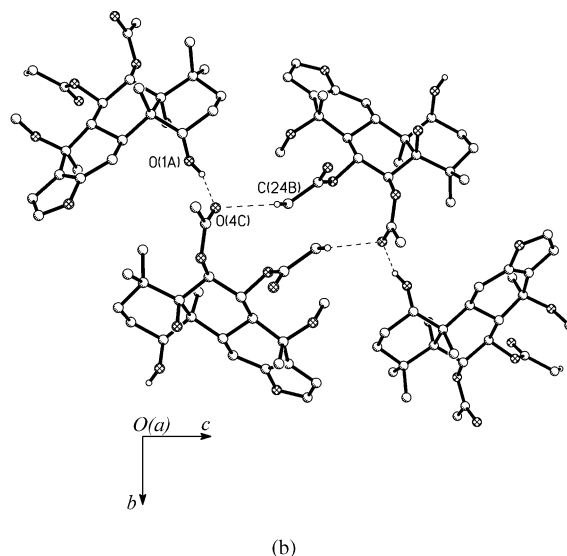
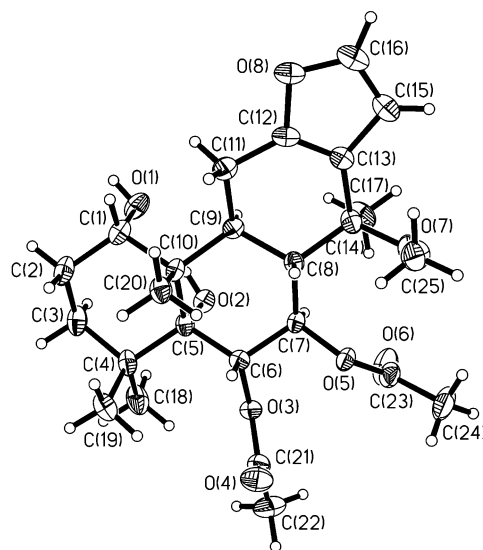


**Figure 6.** (a) Molecular structure of **6**. The C and O atoms are drawn as 30% thermal ellipsoids. (b) Hydrogen-bonding network of **6** viewed roughly down the  $a$ -axis. Selected hydrogen atoms highlight the scheme of hydrogen bonding.

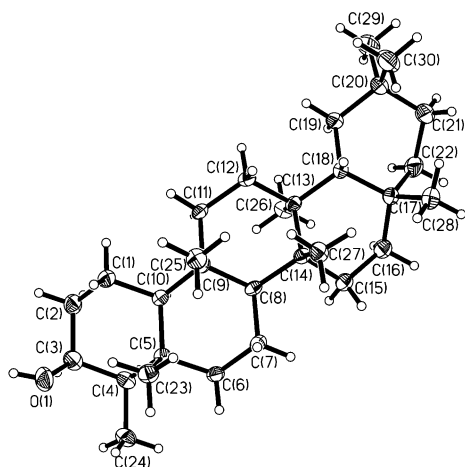


**Figure 7.** Molecular structure of **8**. The C and O atoms are drawn as 30% thermal ellipsoids.

previously, but with low precision ( $R=0.17$  for 2651 reflections).<sup>20</sup> Compound **8** also occurs in many plants;<sup>8</sup> however, it is a reduction derivative of **7** in this context. The wide distribution of **7** and **8** in combination with their low biological activity prompted a presumption that such triterpenoids might serve as a hydrophobic coating during plant evolution and as the precursors of the highly oxygenated and biologically active triterpenoids.<sup>21</sup>

It is interesting to investigate the factors governing the reduction of cassane furanoditerpenoids and friedelane triterpenoids. The reduction of polyacetyl cassane furanoditerpenoid is influenced by the steric hindrance induced by the substituent patterns at C-14. When there is a large substituent, for example,  $\text{CH}_3$  of **9** or  $\text{OCH}_3$  of **11**, at the quasi-equatorial position of ring C (the same orientation as the  $7\beta\text{-OAc}$ ), only the 1-OAc group will be reduced, whereas when the substituent is small, for example, OH of compound **10**, all three acetyl groups will be reduced. It can also be seen that the acetyl group at C-1, occupying the axial position and possessing the smallest steric hindrance, is more easily reduced than those adopting the equatorial positions at C-6 and C-7. Normally,  $\text{LiAlH}_4$  reduction of unhindered cyclohexanones occurs mainly by axial attack, producing the equatorial alcohol,<sup>22</sup> whereas in the case of **7** possessing a C-5 axial methyl group, the result is altered to produce the axial alcohol with an equatorial attack.

Structural optimization using density functional theory (DFT)<sup>23</sup> was used to compare the energies of **4** (reduction product from **9**), and its 6-OH (**4a**) and 7-OH (**4b**) derivatives (**4a** and **4b** were modeled from **9**). The calculations starting with X-ray coordinates were performed using the Gaussian 98 software package<sup>24</sup> (B3LYP based DFT with 6-31G(d) basis set and double-zeta plus polarization function on a heavy atom). The results showed that **4b** is more stable with a ground state energy 7.23 kJ/mol lower than that of **4** and 12.49 kJ/mol lower than **4a** (Fig. 8). The same computation on epifriedelinol (**8**) and friedelinol (**8a**, friedelin- $3\alpha\text{-ol}$ , modeled from **7**) showed that **8a** is more stable by 2.95 kJ/mol (Fig. 9). It can be

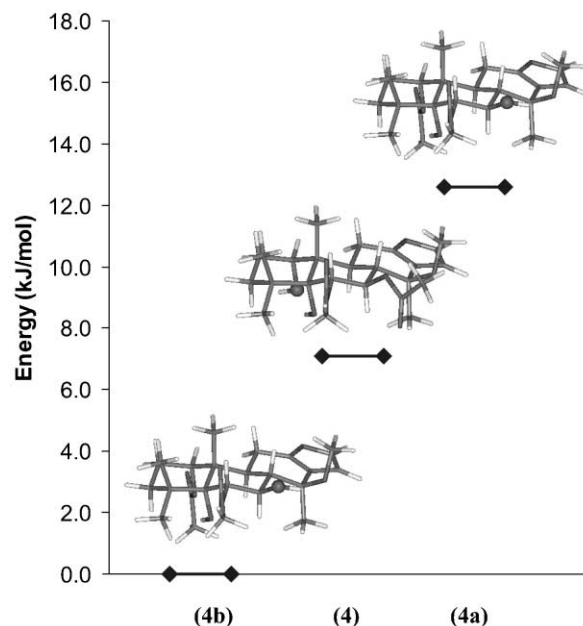


**Figure 8.** DFT-based structural optimization of **4**, **4a** (6-OH derivative) and **4b** (7-OH derivative). Molecule **4b** is more stable with a ground state energy 7.23 kJ/mol lower than **4** and 12.49 kJ/mol lower than (**4a**).

seen that the reduction products are not the ones bearing the lowest energy. Thus the reduction of cassane furanoditerpenoids and friedelane triterpenoids by  $\text{LiAlH}_4$  are dictated by steric control rather than energetic preference.

#### Anti-para3 activity

Compounds **2–8** were evaluated for their inhibitory effects on the para3 virus in vitro by CPE reduction assay according to an established procedure.<sup>25</sup> (Table 3) The furanoditerpenoid lactones **2–3** showed moderate activity against para3 virus and exhibited high toxicity with TI values of 2.8 and 2.7, respectively. Reduction of the acetoxyl group significantly decreased the activity by comparing the  $\text{IC}_{50}$  values of compounds **4–6** with the corresponding parent furanoditerpenoids **9–11**.<sup>4</sup> It is

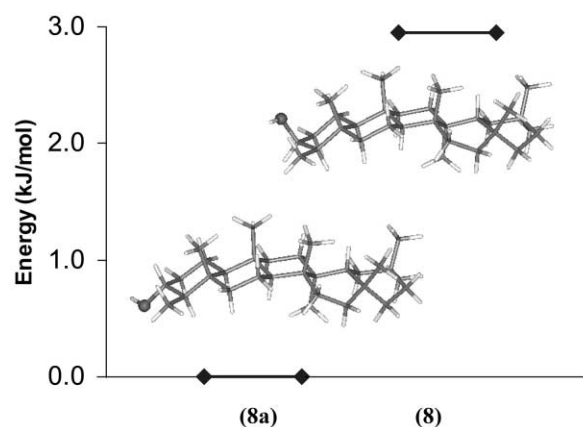


**Figure 9.** DFT-based structural optimization of **8** and **8a** (friedelin- $3\alpha\text{-ol}$ ). Molecule **8a** is more stable than **8** by 2.95 kJ/mol.

**Table 3.** Inhibitory effects of compounds **2–8** on the para3 virus induced cytopathogenicity

Compounds	IC <sub>50</sub> (M×10 <sup>-5</sup> )	TC <sub>50</sub> (M×10 <sup>-5</sup> )	TI
<b>2</b>	5.5	15.6	2.8
<b>3</b>	4.8	12.9	2.7
<b>4</b>	5.2	37.9	7.3
<b>5</b>	6.1	48.9	8.0
<b>6</b>	6.4	120.0	18.8
<b>7</b>	14.0	42.3	3.0
<b>8</b>	12.5	41.0	3.3
Ribavirin	1.0	24.0	24.0

noteworthy that the toxicity of compound **6** is significantly smaller than other compounds with a TI value comparable to its parent furanoditerpenoid **11**.<sup>4</sup> The high hydrophobic friedelane triterpenoids **7–8** were inactive for para3 virus.

Acute respiratory viral infections have long been recognized as important contributors to morbidity and mortality in young children and older adults.<sup>26</sup> The search of natural products as antiviral agents against respiratory viruses, for example respiratory syncytial virus<sup>27</sup> and influenza virus,<sup>28</sup> has attracted recent attention; however, natural products against para3 virus have been less studied. Although the mechanisms of action of furanoditerpenoids are still under investigation, the results achieved so far showed useful clue to develop new antiviral agents against para3 virus from this plant.

### Conclusions

A number of conclusions may be drawn from this work: (i) Three cassane furanoditerpenoids were isolated from the seed of *C. minax*: compound **1** represents the first tetracyclic furanoditerpenoid possessing a 17-methyl attached to a non-oxygenated C-14 from this plant, compound **2** provides a new example of pseudopolymorphism through crystallization from variable mixing ratios of a two-component solvent system, and compound **3** is the only furanoditerpenoid isolated from two different plants in the same genus. (ii) Isolation of friedelane triterpenoid **7** in good yield (0.02%) provides a new rich source and an easy methodology. Notwithstanding its poor bioactivity, its can be used as a precursor to synthesize other physiologically active triterpenoids.<sup>20</sup> (iii) In order to investigate the influence of molecular polarity on antiviral activity, four derivatives **4–6** and **8** were obtained by reduction of **9–11** and **7**, respectively, and the factors governing the reduction of cassane furanoditerpenoids and friedelane triterpenoids were investigated using X-ray structural data in combination with density functional theory. (iv) The antiviral activities of **2–8** against para3 were assessed by CPE reduction assay and compared with previously known compounds. The results of this study shed light on the direction of developing antiviral agents by showing that tetracyclic furanoditerpenoids are superior to pentacyclic furanoditerpenoid lactones, and an increase in polarity results in a decrease of activity.

## Experimental

### General

Melting points were determined using a Fisher Scientific instrument and uncorrected. The UV spectra were obtained on a Beckman DU650 spectrophotometer in MeOH. IR spectra were recorded on a Nicolet Impact 420 FT-IR spectrometer. EIMS were recorded on a Finnigan MAT TSQ 7000 instrument. HRLSIMS measurements were made on an APEX 47e FTMS spectrometer. NMR spectra were obtained with a Bruker spectrometer operating at 300 MHz for <sup>1</sup>H and 75 MHz for <sup>13</sup>C, respectively. Chemical shifts are reported in ppm with TMS as the internal standard, and coupling constants are in Hz. Column chromatographies were performed with silica gel (Qingdao Haiyang Chemical Group Co. Ltd., China); TLC was performed on precoated Si gel 60 F<sub>254</sub> plates (0.2 mm thick, Merck) and spots were detected by UV illumination and by spraying with Ehrlich reagent.

**Plant material.** The seed and stem of *C. minax* Hance were collected in Guangxi Province, PR China in September, 1999. The materials were identified at the Institute of Chinese Medicine, The Chinese University of Hong Kong, where the voucher specimen (No. cm-99 for the seed and No. cm-99s for the stem) is preserved.

**Extraction and isolation.** The 95% ethanol extract of seeds of *C. minax* (10 kg) was divided into six fractions as described previously.<sup>4</sup> The chloroform fraction (50 g) was subjected to column chromatography and eluted with hexane/acetone (10:1). Fractions of 150 mL each were taken and 32 fractions collected. Fractions 9, 10 and 11 were combined to afford **2** (50 mg), and recrystallized from hexane/acetone (20:1) at room temperature. Fractions 17 afford **1** (6 mg), and fractions 19 and 20 afford **3** (30 mg). The stem of the same plant (5 kg) were refluxed with methanol to afford a crude extract (67 g), which was then separated between hexane and water. The hexane fraction (23 g) was subjected to column chromatography and eluted with hexane/acetone (15:1). Compound **7** was obtained from fractions 5–7 and recrystallized from acetone/hexane mixture (1.0 g).

**Reduction of compounds 7 and 9–11.** Compound **7** (21.3 mg) was dissolved in anhydrous THF, then 6 mg LiAlH<sub>4</sub> was added to the solution. The solution was stirred for 30 min. After the reaction a few drops of water was added to hydrolyze the excess LiAlH<sub>4</sub> and filtered. The filtrate was condensed in reduced pressure and the residue was recrystallized from acetone to afford 19.3 mg compound **8** (yield 90%). Compounds **9–11** was reduced with the same method as **7**; however, the resulting products of compounds **4** (yield 76%), **5** (yield 85%) and **6** (yield 81%) were recrystallized from methanol solution.

**Compound 1.** Colorless needle-like crystals; IR (KBr) ν<sub>max</sub> 3586, 1740 cm<sup>-1</sup>; UV λ<sub>max</sub><sup>MeOH</sup> 220 nm (log ε 3.72); EIMS *m/z* (relative intensity, %) 376 [M]<sup>+</sup> (24), 316 [M–HOAc]<sup>+</sup> (100), 298 [M–HOAc–H<sub>2</sub>O]<sup>+</sup> (27), 283 [M–HOAc–H<sub>2</sub>O–CH<sub>3</sub>]<sup>+</sup> (27), 265 [M–HOAc–2H<sub>2</sub>O–CH<sub>3</sub>]<sup>+</sup> (21), 108[C<sub>7</sub>H<sub>8</sub>O]<sup>+</sup> (93), 209 [M–C<sub>7</sub>H<sub>8</sub>O–

OAc)(20), HR-LSIMS  $m/z$  [MH]<sup>+</sup> 377.2328, calculated for C<sub>22</sub>H<sub>32</sub>O<sub>5</sub>, requires 377.2319.

**Compound 4.** Mp 192–194 °C, EIMS  $m/z$  (relative intensity, %): 450 [M]<sup>+</sup> (20), 435 [M–CH<sub>3</sub>]<sup>+</sup> (15), 317 [M–CH<sub>3</sub>–2OAc]<sup>+</sup> (22). HR-LSIMS  $m/z$  [MH]<sup>+</sup> 451.2300, C<sub>24</sub>H<sub>34</sub>O<sub>8</sub> requires 451.2314.

**Compound 5.** Mp 224–226 °C, EIMS  $m/z$  (relative intensity, %): 366 [M]<sup>+</sup> (2), 351 [M–CH<sub>3</sub>]<sup>+</sup> (12), 333 [M–CH<sub>3</sub>–H<sub>2</sub>O]<sup>+</sup> (18), 315 [M–CH<sub>3</sub>–2H<sub>2</sub>O]<sup>+</sup> (4), 297 [M–CH<sub>3</sub>–3H<sub>2</sub>O]<sup>+</sup> (3), 279 [M–CH<sub>3</sub>–4H<sub>2</sub>O]<sup>+</sup> (8), 236 [M–2CH<sub>3</sub>–4H<sub>2</sub>O–CO]<sup>+</sup> (100), 109[C<sub>7</sub>H<sub>8</sub>OH]<sup>+</sup> (27).

HR-LSIMS  $m/z$  [MH]<sup>+</sup> 367.2104, C<sub>20</sub>H<sub>30</sub>O<sub>6</sub>, requires 367.2112.

**Compound 6.** Mp 248–250 °C, EIMS  $m/z$  (relative intensity, %): 464 [M]<sup>+</sup> (17), 432 [M–CH<sub>3</sub>OH]<sup>+</sup> (3), 373 [M–CH<sub>3</sub>OH–OAc]<sup>+</sup> (18), 312 [M–CH<sub>3</sub>OH–2OAc]<sup>+</sup> (18), 138 [C<sub>7</sub>H<sub>7</sub>O+OCH<sub>3</sub>]<sup>+</sup> (100). HR-LSIMS  $m/z$  [MH]<sup>+</sup> 465.2472, C<sub>25</sub>H<sub>36</sub>O<sub>8</sub> requires 465.2478.

**Single crystal X-ray analysis.** The X-ray intensities of 2(2)·H<sub>2</sub>O, 3(2)·C<sub>6</sub>H<sub>14</sub>, 4, 2(5)·0.5H<sub>2</sub>O, 6, 7 and 8 were measured over a hemisphere of reciprocal space, by a combination of three sets of exposures on a Bruker

**Table 4.** Crystal data and structure refinement parameters

Compound	2(1)·H <sub>2</sub> O	3(2)·C <sub>6</sub> H <sub>14</sub>	(4)
CCDC deposit no.	175941	175942	175943
Color/shape	Colorless/needle	Colorless/prism	Colorless/prism
Crystal dimensions (mm <sup>3</sup> )	0.67×0.12×0.09	0.65×0.26×0.18	0.61×0.25×0.17
Chemical formula	2C <sub>22</sub> H <sub>32</sub> O <sub>5</sub> ·H <sub>2</sub> O	3C <sub>22</sub> H <sub>28</sub> O <sub>6</sub> ·C <sub>6</sub> H <sub>14</sub>	C <sub>24</sub> H <sub>34</sub> O <sub>8</sub>
Formula weight	770.96	1251.57	450.51
Temperature (K)	293(2)	293(2)	293(2)
Crystal system	Orthorhombic	Orthorhombic	Monoclinic
Space group	P2 <sub>1</sub> 2 <sub>1</sub> 2 <sub>1</sub> (No. 19)	P2 <sub>1</sub> 2 <sub>1</sub> 2 <sub>1</sub> (No. 19)	P2 <sub>1</sub> (No. 4)
Unit cell dimensions	<i>a</i> = 8.817(1) Å <i>b</i> = 10.112(2) Å <i>c</i> = 46.686(9) Å	<i>a</i> = 8.7592(7) Å <i>b</i> = 19.732(1) Å <i>c</i> = 37.815(3) Å	<i>a</i> = 10.0824(8) Å <i>b</i> = 9.6405(8) Å <i>c</i> = 11.897(1) Å β = 100.285(2)
Volume (Å <sup>3</sup> )	4162.6(14)	6535.9(9)	1137.8(1)
Z	4	4	2
Density (calculated) (mg/m <sup>3</sup> )	1.227	1.258	1.315
Absorption coefficient (mm <sup>-1</sup> )	0.087	0.090	0.098
Diffractometer/scan	Bruker SMART 1000 CCD/ω	Bruker SMART 1000 CCD/ω	Bruker SMART 1000 CCD/ω
θ range (°)	1.74–25.20	1.92–25.00	1.74–25.03
Reflections measured	22582	36615	6175
Independent reflections ( <i>R</i> <sub>int</sub> )	7416 (0.1818)	11516 (0.0522)	3889(0.0696)
Observed reflections	3014	6963	3226
Data/restraints/parameters	7416/0/491	11516/0/782	3889/1/289
Extinction coefficient	0.0178(17)	0.0007(3)	0.000(2)
Goodness of fit on F <sup>2</sup>	0.909	0.995	0.990
Final <i>R</i> indices [I > 2σ(I)]	0.0794	0.0611	0.0588
<i>R</i> indices (all data)	0.1964	0.1098	0.0694
2(5)·0.5H <sub>2</sub> O	<b>6</b>	<b>7</b>	<b>8</b>
175944	175945	175946	175847
Colorless/block	Colorless/block	Colorless/needle	Colorless/block
0.58×0.33×0.24	0.63×0.24×0.17	0.62×0.12×0.09	0.53×0.34×0.27
2C <sub>20</sub> H <sub>30</sub> O <sub>6</sub> ·0.5H <sub>2</sub> O	C <sub>25</sub> H <sub>36</sub> O <sub>8</sub>	C <sub>30</sub> H <sub>50</sub> O	C <sub>30</sub> H <sub>52</sub> O
741.89	464.54	426.70	428.72
293(2)	293(2)	293(2)	293(2)
Tetragonal	Orthorhombic	Orthorhombic	Monoclinic
P4 <sub>2</sub> (No. 77)	P2 <sub>1</sub> 2 <sub>1</sub> 2 <sub>1</sub> (No. 19)	P2 <sub>1</sub> 2 <sub>1</sub> 2 <sub>1</sub> (No. 19)	C2 (No. 5)
<i>a</i> = 16.764(2) Å	<i>a</i> = 6.9582(8) Å <i>b</i> = 16.492(1) Å <i>c</i> = 20.840(2) Å	<i>a</i> = 6.3794(6) Å <i>b</i> = 13.936(1) Å <i>c</i> = 28.425(3) Å	<i>a</i> = 13.440(1) Å <i>b</i> = 6.4089(5) Å <i>c</i> = 29.594(2) Å β = 92.290(2)
<i>c</i> = 13.267(3) Å			
3728.5(11)	2391.4(5)	2527.1(4)	2547.1(3)
4	4	4	4
1.322	1.290	1.122	1.118
0.097	0.095	0.065	0.064
Bruker SMART	Bruker SMART	Bruker SMART	Bruker SMART
1000 CCD/ω	1000 CCD/ω	1000 CCD/ω	1000 CCD/ω
1.21–25.04	1.57–25.04	1.43–24.99	1.38–25.03
20348	12954	13762	6912
6561 (0.0542)	4232 (0.0582)	4457(0.0815)	4066 (0.0277)
4828	2872	2194	3629
6561/1/475	4232/0/300	4457/0/281	4066/1/280
0.0013(4)	0.008(9)	0.0032(6)	0.000(3)
0.958	0.907	0.908	1.039
0.0445	0.0399	0.0501	0.0442
0.0656	0.0655	0.1343	0.0495

SMART1000 CCD diffractometer. The intensities were corrected for Lorentz and polarization effects but not for absorption. The structures were solved by direct methods and refined by full-matrix least-squares on  $F^2$  using SHELXTL-97 software package.<sup>29</sup> The crystallographic data of the above compounds are shown in Table 4. Among these crystal structures, 2(1)·H<sub>2</sub>O has one very long unit-cell axis and the crystals occur as very slim needles, so that the diffraction patterns are weak. Furthermore, the water molecule is disordered over two positions in the asymmetric unit, being represented by O-1w with a site occupancy factor (sof)=0.7 and O-2w with sof=0.3; thus the R indices of the hemihydrate of (1) are higher than usual. In addition, the solvent molecule (hexane) in 3(2)·C<sub>6</sub>H<sub>14</sub> exhibited large thermal motion and were refined isotropically.

#### Antiviral assay

Para3 virus and HEP-2 cells were obtained from American Type Culture Collection. Dulbecco's modified eagle's medium was purchased from Sigma Company, USA. Fetal bovine serum was obtained from Biofluids Inc., USA.

The antiviral experiments were performed in 96-well microtiter plates using the procedures described previously.<sup>25</sup> Ribavirin was used as a positive control, and an infection control was made in the absence of samples. A fixed quantity of para3 virus in suspension was added to the monolayers of HEP-2 cells, and the cytopathogenic effects (CPE, loss of monolayer, rounding, shrinking of the cells, granulation, and vacuolization in the cytoplasm) were observed under an inverted microscope. The concentration that reduced CPE by 50% with respect to virus control was defined as IC<sub>50</sub>. The concentration that showed 50% cytotoxic effect was defined as TC<sub>50</sub>. Both IC<sub>50</sub> and TC<sub>50</sub> were expressed in M (mol/L). The selectivity against Para3 virus was characterized by the therapeutic index (TI) = TC<sub>50</sub>/IC<sub>50</sub>. The antiviral activity of compound 1 was not measured due to the limited amount of available sample.

**Supporting information available.** Crystal data in standard CIF format have been deposited with the Cambridge Crystallographic Data Centre with CCDC number shown in Table 4. Copies of the data can be obtained, free of charge, on application to CCDC, 12 Union Road, Cambridge CB2 1EZ, UK (Fax: +44-1223-336033; e-mail: deposit@ccdc.cam.ac.uk). Comparison of the equivalent displacement parameters, bond distances, bond angles and torsion angles for the two independent molecules in 2(1)·H<sub>2</sub>O, three independent molecules in 3(2)·C<sub>6</sub>H<sub>14</sub> and two independent molecules in 2(5)·0.5H<sub>2</sub>O are listed in Tables S1, S2 and S3, respectively; see supplementary materials.

#### Acknowledgements

This work is partially supported by Hong Kong Research Grant Council Earmarked Grants CUHK 4206/99P and CUHK 4171/99M and Industrial Support

Fund AF/281/97 from the Hong Kong SAR Government. We thank Dr. Zhi-Feng Liu for helpful discussions regarding the structural optimizations.

#### References and Notes

- (a) Newman, D. J.; Cragg, G. M.; Snader, K. M. *Nat. Prod. Rep.* **2000**, *17*, 215. (b) Matthée, G.; Wright, A. D.; König, G. M. *Planta Med.* **1999**, *65*, 493. (c) Brady, S. F.; Singh, M. P.; Janso, J. E.; Clardy, J. *J. Am. Chem. Soc.* **2000**, *122*, 2116. (d) Henkel, T.; Brumme, R. M.; Müller, H.; Reichel, F. *Angew. Chem. Int. Ed.* **1999**, *38*, 643.
- Treanor, J.; Falsey, A. *Antiviral Res.* **1999**, *44*, 79.
- Jiangsu New Medical College. *Dictionary of Chinese Traditional Medicine*; Shanghai People's Publishing House: PR China, 1986; p 1289.
- Jiang, R. W.; Ma, S. C.; But, P. P. H.; Mak, T. C. W. *J. Nat. Prod.* **2001**, *64*, 1266.
- Jiang, R. W.; But, P. P. H.; Ma, S. C.; Mak, T. C. W. *Phytochemistry* **2001**, *57*, 517.
- Peter, S. R.; Tinto, W. F.; Mclean, S.; Reynolds, W. F.; Yu, M. *J. Nat. Prod.* **1997**, *60*, 1219.
- (a) Lin, M. T.; Chen, L. C.; Chen, C. K.; Liu, K. C. S. C.; Lee, S. S. *J. Nat. Prod.* **2001**, *64*, 707. (b) Wu, T. S.; Chan, Y. Y.; Leu, Y. L. *Chem. Pharm. Bull.* **2000**, *48*, 1006. (c) Del, R. C. M.; Mata, R.; Castaneda, P.; Kirby, G. C.; Warhurst, D. C.; Croft, S. L.; Phillipson, J. D. *Planta Med.* **2000**, *66*, 463.
- (a) Huang, H. C.; Shen, C. C.; Chen, C. F.; Wu, Y. C.; Kuo, Y. H. *Chem. Pharm. Bull.* **2000**, *48*, 1079. (b) Queiroga, C. L.; Silva, G. F.; Dias, A. P.; Carvalho, J. E. D. *J. Ethnopharm.* **2000**, *72*, 465.
- Galasso, G. J.; Merigan, T. C.; Buchanan, R. A. *Antiviral Agents and Viral Diseases of Man*, 2nd ed.; Raven Press, New York, 1984; p 313.
- Kitagawa, I.; Simanjuntak, P.; Watano, T.; Shibuya, H.; Fujii, S.; Yamagata, Y.; Kobayashi, M. *Chem. Pharm. Bull.* **1994**, *42*, 1798.
- Collings, J. C.; Roscoe, K. P.; Thomas, R. L. I.; Batsanov, A. S.; Stimson, L. M.; Howard, J. A. K.; Marder, T. B. *New J. Chem.* **2001**, *25*, 1410.
- (a) For examples from *Caesalpinia* genus, see: Ashok, D. P.; Alan, J. F.; Lee, W.; Gary, Z.; Rex, R.; Mark, F. B.; Leo, F.; Randall, K. J. *Tetrahedron* **1997**, *53*, 1583. (b) Peter, S. R.; Tinto, W. F.; McLean, S.; Reynolds, W. F.; Yu, M. *J. Nat. Prod.* **1997**, *60*, 1219. (c) Peter, S. R.; Tinto, W. F.; Mclean, S.; Reynolds, W. F.; Tay, L. L. *Tetrahedron. Lett.* **1997**, *38*, 5767. (d) Lyder, D. L.; Peter, S. R.; Tinto, W. F.; Bissada, S. M.; Mclean, S.; Reynolds, W. F. *J. Nat. Prod.* **1998**, *61*, 1462. (e) Kinoshita, T. *Chem. Pharm. Bull.* **2000**, *48*, 1375.
- (a) For examples from *Pterodon* genus, see: Mahajan, J. R.; Monteiro, M. B. *J. Chem. Soc., Perkin Trans. 1* **1973**, *5*, 520. (b) Campos, A. M.; Silveira, E. R.; Raimudo, B. F.; Teixeira, T. C. *Phytochemistry* **1994**, *36*, 403. (c) Antonio, J. D.; Luiz, C. A. B.; Dorila, P. V.; Dalton, L. F. A. *J. Nat. Prod.* **1996**, *59*, 770.
- Polhill, R. M.; Raven, P.H. *Advances in Legume Systematics*; Royal Botanical Gardens: Richmond, Surrey TW9 3AE, UK, 1981; p 81 and p 231.
- Karin, B. B.; George, F. *Acta Cryst.* **1969**, *B* (25), 720.
- Nangia, A.; Desiraju, G. R. *Chem. Commun.* **1999**, 605.
- Thaimattam, R.; Xue, F.; Sarma, J. A. P.; Mak, T. C. W.; Desiraju, G. R. *J. Am. Chem. Soc.* **2001**, *123*, 4432.
- (a) Taylor, R.; Kennard, O. *J. Am. Chem. Soc.* **1982**, *104*, 5063. (b) Thomas, S. *J. Chem. Soc., Chem. Comm.* **1997**, 727. (c) Desiraju, G. R.; Steiner, T. *The Weak Hydrogen Bond in Structural Chemistry and Biology*; Oxford University Press: New York, 1999.

19. (a) Mahato, S. B.; Kundu, A. P. *Phytochemistry* **1994**, *37*, 1517. (b) Declercq, J. P.; Puyvelde, L. V.; Kimpe, N. D.; Nagy, M.; Verhegge, G.; Vierman, R. D. *Acta Cryst. C* (47), 209.
20. Laing, M.; Burke-Laing, M. E.; Bartho, R.; Weeks, C. M. *Tetrahedron Lett.* **1977**, *43*, 3839.
21. Corey, E. J.; Ursprung, J. J. *J. Am. Chem. Soc.* **1956**, *78*, 5041.
22. Wigfield, D. C. *Tetrahedron* **1979**, *35*, 449.
23. Beck, A. D. *J. Chem. Phys.* **1993**, *98*, 5648.
24. Frisch, M. J.; Trucks, G. W.; Schlegel, H. B.; Scuseria, G. E.; Robb, M. A.; Cheeseman, J. R.; Zakrzewski, V. G.; Montgomery, Jr., J. A.; Stratman, R. E.; Burant, J. C.; Dapprich, S.; Millam, J. M.; Daniels, A. D.; Kudin, K. N.; Strain, M. C.; Farkas, O.; Tomasi, J.; Barone, V.; Cossi, M.; Cammi, R.; Mennucci, B.; Pomelli, C.; Adamo, C.; Clifford, S.; Ochterski, J.; Peterson, G. A.; Ayala, P. Y.; Cui, Q.; Morokuma, K.; Malick, D. K.; Rabuck, A. D.; Raghavachari, K.; Foresman, J. B.; Cioslowski, J.; Ortiz, J. V.; Baboul, A. G.; Stefabov, B. B.; Liu, G.; Liashenko, A.; Piskorz, P.; Komaromi, I.; Gomperts, R.; Martin, R. L.; Fox, D. J.; Keith, T.; Al-Laham, M. A.; Peng, C. Y.; Nanayakkara, A.; Challacombe, M.; Gill, P. M. W.; Johnson, P.; Chen, W.; Wong, M. W.; Andres, J. L.; Gonzalez, C.; Head-Gordon, M.; Replogle, E. S.; Pople, J. A. *Gaussian 98*, revision A.9; Gaussian: Pittsburgh, PA, 1998.
25. (a) Piraino, F.; Brandt, C. R. *Antiviral Res.* **1999**, *43*, 67. (b) Ma, S. C.; He, Z. D.; Deng, X. L.; But, P. P. H.; Ooi, V. E. C.; Xu, H. X.; Lee, S. H. S.; Lee, S. F. *Chem. Pharm. Bull.* **2001**, *49*, 1471. (c) Jiang, R. W.; Ma, S. C.; But, P. P. H.; Mak, T. C. W. *J. Chem. Soc., Perkin Trans. 1* **2001**, 2920. (d) Jiang, R. W.; But, P. P. H.; Ma, S. C.; Ye, W. C.; Chan, S. P.; Mak, T. C. W. *Tetrahedron Lett.* **2002**, *43*, 2415–2418.
26. Ryan, K. J. *Sherris Medical Microbiology, An Introduction to Infectious Diseases*, 3rd ed.; Appleton and Lange, Norwalk, 1994; p 451.
27. (a) Piraino, F.; Brandt, C. R. *Antiviral Res.* **1999**, *43*, 67. (b) Chen, J. L.; Blanc, P.; Stoddart, C. A.; Bogan, M.; Rozhon, E. J.; Parkinson, N.; Ye, Z. J.; Cooper, R.; Balick, M.; Nanakorn, W.; Kernan, M. R. *J. Nat. Prod.* **1998**, *61*, 1295.
28. Nagai, T.; Suzuki, Y.; Tomimori, T.; Yamada, H. *Biol. Pharm. Bull.* **1995**, *18*, 295.
29. Sheldrick G. M. *SHELXTL, version 5.1*, Structure Determination Software Programs package, Bruker Analytical X-ray Systems: Madison, WI, USA, 1997. This program mainly consists of (i) XPREP (space group determination), (ii) XS (structure elucidation), (iii) XL (structure refinement) and (iv) XP (graphic display).